



Universiteit
Leiden
The Netherlands

Single cell biochemistry to visualize antigen presentation and drug resistance

Griekspoor, A.C.

Citation

Griekspoor, A. C. (2006, November 1). *Single cell biochemistry to visualize antigen presentation and drug resistance*. Retrieved from <https://hdl.handle.net/1887/4962>

Version: Corrected Publisher's Version

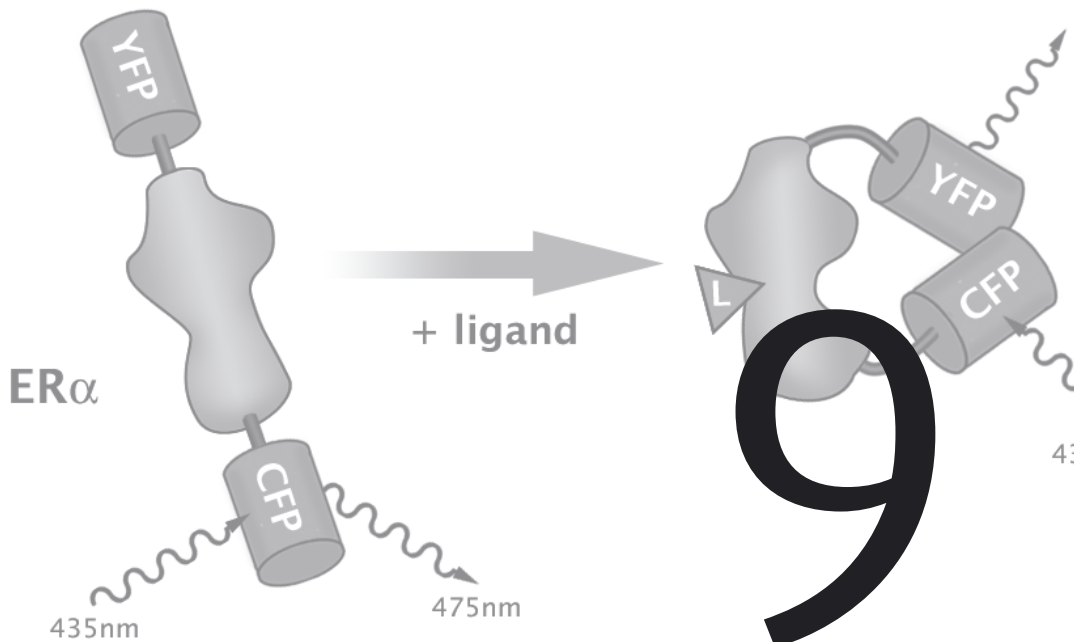
License: [Licence agreement concerning inclusion of doctoral thesis in the Institutional Repository of the University of Leiden](#)

Downloaded from: <https://hdl.handle.net/1887/4962>

Note: To cite this publication please use the final published version (if applicable).

Tamoxifen resistance by a conformational arrest of the estrogen receptor α after PKA activation in breast cancer

Reprinted from Cancer Cell, vol. 5: 597–605,
Copyright (2004), with permission from Elsevier



Tamoxifen resistance by a conformational arrest of the estrogen receptor α after PKA activation in breast cancer

Alexander Griekspoor^{*1}, Rob Michalides^{*1}, Astrid Balkenende¹, Desiree Verwoerd¹, Lennert Janssen¹, Kees Jalink², Arno Floore³, Arno Velds⁴, Laura van 't Veer³ and Jacques Neefjes¹

¹Division of Tumour Biology, The Netherlands Cancer Institute, Amsterdam, The Netherlands.

²Division of Cell Biology, The Netherlands Cancer Institute, Amsterdam, The Netherlands.

³Division of Experimental Therapy, The Netherlands Cancer Institute, Amsterdam, The Netherlands.

⁴Central Microarray Facility, The Netherlands Cancer Institute, Amsterdam, The Netherlands.

Using a novel approach that detects changes in the conformation of ER α , we studied the efficacy of anti-estrogens to inactivate ER α under different experimental conditions. We show that phosphorylation of serine-305 in the hinge region of ER α by protein kinase A (PKA) induced resistance to tamoxifen. Tamoxifen bound but then failed to induce the inactive conformation, invoking ER α -dependent transactivation instead. PKA activity thus induces a switch from antagonistic to agonistic effects of tamoxifen on ER α . In clinical samples, we found that downregulation of a negative regulator of PKA, PKA-R1 α , was associated with tamoxifen resistance prior to treatment. Activation of PKA by downregulation of PKA-R1 α converts tamoxifen from an ER α inhibitor into a growth stimulator, without any effect on ICI 182,780 (Fulvestrant).

CORRESPONDENCE

Rob J. A. M. Michalides
Division of Tumour Biology
The Netherlands Cancer
Institute
Plesmanlaan 121
1066 CX Amsterdam
The Netherlands
Tel.: +31 20 512 2022
Fax: +31 20 512 2029
E-mail: r.michalides@nki.nl

Significance

Estrogen receptor-positive breast cancer patients are commonly treated with the anti-estrogen tamoxifen, which gives a 50% reduction in recurrence. Here, we describe that inactivation of the estrogen receptor by anti-estrogens leads to rapid conformational changes in the receptor, which can be followed by FRET (fluorescence resonance energy transfer). Using this method, we can determine the efficacy of two different anti-estrogens, tamoxifen and Fulvestrant. Breast cancers resistant to tamoxifen are often still sensitive to Fulvestrant. We demonstrate that resistance to tamoxifen is mediated by a modification of the estrogen receptor by

protein kinase A, not only in experimental setting, but in breast cancer patients as well. This modification converts the antagonist tamoxifen into an agonist, reversing its effect on tumor cell growth.

Introduction

Approximately 70% of all breast cancers are dependent for their growth on estrogen and on a functional estrogen receptor α (ER α). Hence, ER-positive breast cancer is usually treated with hormone reduction or anti-estrogens (1). The most commonly used anti-estrogen is tamoxifen, and it has been calculated that about one million years of life are saved by tamoxifen per year in the developed countries (2). Still, only half of the recurrences in ER+ breast tumors respond to tamoxifen, while the other half show resistance. Mutations in ER that lead

* A. Griekspoor and R. Michalides contributed equally to this paper

to resistance are rarely found in patients (3), whereas multiple other mechanisms have been associated with tamoxifen resistance *in vitro*. Reported are: phosphorylation of the ER α by protein kinase A (PKA) (4) or MAP-kinase (5), overexpression of c-erbB2 (6), EGF-R or SRC-1 (7), and stabilization of the interaction between ER α and SRC-1 by cyclin D1 (8) and cyclin A-CDK2 (9). Whether these mechanisms are operational in tamoxifen-resistant breast cancer is unclear. Understanding the mechanism of tamoxifen resistance in ER+ breast cancers should allow early identification of these tumors and adaptation of the treatment before more aggressive cells arise.

ER α is a member of the nuclear hormone receptor superfamily and regulates transcription of ER-specific target genes in response to the hormone estradiol (E2) (10). ER α contains several functional domains, including a centrally located DNA binding domain connected through a hinge region to a C-terminal ligand binding domain (LBD) that binds the agonist estradiol, but also antagonists such as tamoxifen and ICI-182,780 (commercial name: Faslodex or Fulvestrant). Hormone binding results in rapid dissociation from chaperone proteins, leading to binding of an ER homodimer to its cognate estrogen responsive element (ERE) binding site on the DNA. This initiates transcription by recruiting the basal transcription machinery through a variety of coactivators, including steroid receptor cofactor-1 (SRC-1) and AIB1 (11). It is this recruitment that is inhibited by anti-estrogens.

The conformation of the LBD of ER is affected by ligand binding (12-15). Estradiol binding affects the conformation of helix12 of the LBD such that coactivators are recruited and transcription ensues. Anti-estrogens like tamoxifen and ICI-182,780 bind to the same site (16), but induce a reorientation of this particular helix, thereby preventing the interaction with coactivators and inhibiting ER-driven transcription. Yet, the effects of the individual anti-estrogens are not identical (17-19). For example, a fraction of ER-positive tamoxifen resistant breast tumors is still sensitive to ICI-182,780 *in vitro* as well as *in vivo* in patients (17, 20-22). The fact that estrogen and anti-estrogens induce different ER conformations was the rationale behind designing a fluorescence resonance energy transfer (FRET) probe that can monitor these conformations in living cells (23).

Experimental Procedures

Cell culture, transfection, and ERE-luciferase reporter assays

U2OS and T47D cells were cultured in DMEM medium in the presence of 10% FCS and standard antibiotics. U2OS cells containing ER constructs were cultured in phenol red-free DMEM medium containing 5% charcoal treated serum (CTS, Hyclone). For the FRET experiments, cells were cultured on 2 cm round glass coverslips, and at the times indicated estradiol (Sigma), 4-OH-tamoxifen (Sigma), or ICI-182,780 (Tocris) was added at the concentrations indicated. Forskolin (Sigma) was added 15 min prior to measurements at a final concentration of 10^{-5} M. For the ERE-luciferase experiments, 10^{-7} M estrogen or anti-estrogen was added to the medium after transfection, followed by culturing the cells for 48 hr before harvesting. For transient transfections, 4×10^5 U2OS cells were plated in a 6-well plate culture dish and cultured overnight. The cells were transfected with 1 μ g of expression vectors pCMV-cyclin D1, pCMV-SRC-1 (24), and 0.4 μ g of pcDNA3-YFP-ER-CFP (see below) using Transfast reagents (Promega) following the manufacturer's protocol. For ERE-luciferase reporter assays, cells were transfected with 1 μ g ERE-Tk-Firefly luciferase (25) and 1 ng of SV40 Renilla luciferase construct, and cells were incubated under the conditions indicated for 48 hr. The luciferase assay was performed as described (25).

Fluorescence resonance energy transfer (FRET)

For FRET experiments, cells on coverslips were placed on an inverted Zeiss Axiovert 135 microscope equipped with a dry Achroplan 63x objective. FRET equipment was as described previously (26). CFP was excited at 432 ± 5 nm and emission of YFP was detected at 527 nm and CFP at 478 nm. FRET was expressed as ratio of YFP to CFP signals. The ratio was arbitrarily set as 1.0 at the onset of the experiment. Changes are expressed as percent deviation from this initial value of 1.0. For data acquisition, Felix software (PTI Inc.) was used.

YFP-ER-CFP constructs and *in vitro* phosphorylation

The pCMV-ER α construct was obtained from P. Chambon (Strasbourg). A fusion construct was made by ligation of PCR products from ER α and CFP in-frame in the YFP-PH pcDNA3vector (26). We used primer 5'CCCAGAATCAATGACCTCCACACCAAAGCATCT, creating an *EcoRI* site, and 5'CCCACCTCGAGGAC TGTGGCAGGGAAACCCTCT, eliminating the stop codon of ER α , and introduced a *XhoI* site compatible with the 5' *SalI* site from CFP (sequence 5'CCCA GTCGACATGGTGAGCAAGGGCGAGGA), while a stop

codon was introduced at the 3' end (5'CCCATCTAGATC ACTTGACAGCTCGTCCATG). The single fluorescent protein containing ER α constructs (YFP-ER α and ER α -CFP) was constructed in an identical manner. Site-directed mutagenesis of serine-236 and -305 to alanine was performed with the YFP-ER α -CFP construct as a template using the appropriate modified oligonucleotides. All constructs were verified by sequence analysis using 4Peaks (mekentosj.com). The pcDNA3-YFP-ER α -CFP construct was transfected in U2OS cells, and after 48 hr, cells were inspected by confocal microscopy for YFP emission at 500–565 nm. Protein expression was examined by Western blotting using antibodies against ER- α (Stressgen Biotechnologies Corp) and GFP (27) and detected using an ECL detection kit (Amersham).

The *in vitro* protein kinase A assay was performed as described before (28). Briefly, equal amounts of protein of wt and Ser 236 or -305 mutants of immunopurified YFP-ER α -CFP were incubated with 10 units of bovine protein kinase A catalytic subunit (Sigma) and $\gamma^{32}\text{P}$ -ATP for 30 min at 30°C, under conditions provided by the supplier. Half of the reaction was evaluated by autoradiography after SDS-PAGE gelelectrophoresis, the other half by Western blotting using antibody against GFP.

pSUPER-PKA-R1 α construct and *in vitro* proliferation

To generate the pSUPER-PKA-R1 α , the RNAi vector pSUPER (29) was digested with *Bgl*II and *Hind*III and the annealed oligos containing the sequence GGGGATAACTTCTATGTGA specific for PKA-R1 α were ligated into the vector. Downregulation of PKA-R1 α was confirmed by Western blotting using anti-PKA-R1 α antibodies (BD Transduction Laboratories Inc).

For *in vitro* proliferation assay with pSUPER-PKA-R1 α , 100,000 single T47D cells were transfected with pSUPER-PKA-R1 α DNA (1 μg) or control empty vector (pSUPER) by electroporation (Biorad) and subsequently cultured in the presence of either CTS medium, 10^{-7} M ICI-182,780 (ICI), 10^{-7} M 4-OH-tamoxifen (TAM), or 10^{-7} M E2 for three weeks. Resulting colonies were stained with Coomassie blue.

Microarray analysis

Patients were participating in the tamoxifen trial (MTAMOX) of the Comprehensive Cancer Center Amsterdam, where no tamoxifen versus one year and three years adjuvant tamoxifen treatment were compared with respect to recurrence-free interval and overall survival in postmenopausal women with stage I-IIIB invasive breast cancer (13). All tumors were ER-

positive by immunohistochemical staining. There were two randomizations: first, between no tamoxifen and tamoxifen, and after one year in the tamoxifen arm, between 1 and 3 years tamoxifen. In this study, only patients in the initial tamoxifen arm were included.

Starting date was date of first randomization, ranging from 10/86 to 11/93. Median follow-up was 132 months (36–168) for the 50 patients without recurrence against 41 months (7–132) for the 20 patients who recurred. As estimated by the inverse survival technique (inverting the role of recurrence/death and censoring in calculating the Kaplan-Meier curve), all patients had a potential follow-up of at least 5 years, 45% a follow-up of at least 9 years, and 25% a follow-up of at least 10 years. Follow-up was closed November 2002.

RNA extraction, amplification, and hybridization

Tumor biopsies were frozen in liquid nitrogen at the time of surgery and stored at -80°C . 30 cryostat sections of 30 μm were cut from the tumor tissue. RNA was isolated from these sections using RNAzol and a polytron homogenizer according to manufacturer's protocol (Campro Scientific, Veenendaal, The Netherlands), followed by DNase treatment. 4 μg of this total RNA was amplified, using a modified Eberwine amplification protocol (<http://microarrays.nki.nl>) yielding an average of 40 μg antisense RNA (aRNA).

All labeling and hybridization protocols are published at <http://microarrays.nki.nl/download/protocols>. 10 μg aRNA from 56 tumors (16 recurrence, 40 nonrecurrence) of this series was pooled to create a reference. 2 μg aRNA of each tumor was primed with random hexamers and labeled with Cy3 or Cy5 in a cDNA reaction, and hybridized on a NKI 18K human cDNA array (<http://microarrays.nki.nl>) against the reference, labeled with the other Cy dye. All hybridizations were done twice; in the second hybridization, the labels were switched (color reverse). Arrays were scanned with a confocal laser scanner (Scanarray 4000 GSI Lumonics).

Array data analysis

Fluorescent intensities from the arrays were quantified with Imagen software (Biodiscovery). After normalization of the Cy3/Cy5 signal (30), an average ratio of the two-color reverse hybridizations for each gene was calculated. Genes were selected that were significantly deregulated in minimally 5 tumors (that is, at least a 2-fold difference and p value < 0.01) (31). For these 6,000 genes, the correlation between the prognostic category (recurrence versus nonrecurrence) and the logarithmic expression ratios for all 70 samples was calculated, and a rank order was made using the Wilcoxon

rank sum test, based on the magnitude of the correlation coefficient (32). After Monte Carlo analysis, a cutoff point of a correlation of 0.37 was chosen. Some 100 genes appeared to have a higher correlation and were thus strongly associated with recurrence. PKA-R1 α was one of these genes with a high correlation (rank order 53), and was shown by a two-sample t test to be significantly downregulated in the group with recurrence compared to the group without recurrences (two-sample t test for combined probes; p value = 0.0000697). The other genes of the PKA pathway included in the array did not show a significant difference between the recurrence and nonrecurrence group (p value > 0.05). All data for the relevant probes is shown in Supplemental Table S2.

Results

FRET marks inactivation of ER α

We generated a recombinant ER α with two variants of the green fluorescent protein: YFP at the N- and CFP at the C terminus (Figure 1A). Any alteration in position or orientation of the CFP and YFP molecules may result in a change in energy transfer between these fluorophores (23, 26). First, we determined whether the YFP/CFP modification affects the normal behavior of ER α . U2OS cells stably transfected with the YFP-ER-CFP construct showed fluorescent nuclei (Figure 1B) containing a 119 kDa YFP-ER-CFP fusion protein, as detected by Western blot analysis with anti-ER and anti-GFP antibodies (Figure 1C). This construct was normally able to induce ERE-mediated transactivation. Culturing the cells with estradiol for 48 hr resulted in a 35-fold increase of ERE-luciferase activity over control cells grown in estrogen-depleted serum (CTS), whereas tamoxifen or ICI-182,780 hardly induced ERE-mediated reporter activity (Figure 1D). These values were comparable to those found using a nonmodified pCMV-ER construct (data not shown), indicating that the GFP modifications did not alter the activity of ER. Moreover, the pCMV-ER wt and the YFP-ER-CFP fusion construct showed comparable IC₅₀ and EC₅₀ values for estradiol, OH-tamoxifen, and ICI-182,780 in transactivation assays (Figures 1E–1G).

Subsequently, we measured conformational changes in ER α by FRET after addition of estradiol (E2) or the anti-estrogens tamoxifen and ICI-182,780. Alterations in the distance or orientation of CFP and YFP will potentially affect energy transfer from CFP to YFP, which can be observed when CFP is excited at 432 nm and the emission of CFP (at 478

nm) and YFP (at 527 nm) is simultaneously measured (Figure 2A). In case of energy transfer, emission of YFP should occur at the expense of CFP (23), and alterations in FRET (fluorescence resonance energy transfer) are depicted as changes in ratio between these two signals. Living U2OS cells transfected with the YFP-ER-CFP construct were assayed in the presence of various combinations of estrogen (E2), tamoxifen, and ICI-182,780 (as indicated in Figures 2B–2D). An alteration in FRET was observed only after addition of tamoxifen or ICI-182,780, and reached completion within 10 min. E2 did not affect FRET, not even when a 10-fold molar excess was added after anti-estrogen addition (Figure 2C). Apparently, the YFP-ER-CFP FRET probe only detected ER inactivation by the anti-estrogens tamoxifen or ICI-182,780, and not activation by E2. Application of the FRET in physiologically more relevant MCF7 and T47D breast cancer cells yielded similar FRET alterations upon addition of OH-tamoxifen and ICI-182,780. Since U2OS cells are more easily transfected, and since we wanted to study initial conformational changes in YFP-ER-CFP in cells devoid of endogenous ER, U2OS cells were used in further FRET studies.

Since ER α forms homodimers, the FRET changes observed could result from inter- or intramolecular energy transfer between CFP and YFP. To investigate this, we examined the FRET changes in U2OS cells that were transfected with either YFP-ER or ER-CFP alone or with equal amounts of both constructs (Figure 2E). No detectable FRET changes occurred upon tamoxifen addition in cells with either YFP-ER or ER-CFP expression alone, nor in cells expressing both constructs. These findings indicated that ER inactivation by anti-estrogens (Figure 2) resulted in an intramolecular change in ER α that can be visualized by FRET.

Resistance to anti-estrogens measured by FRET

The FRET probe was used for assaying conditions that induce resistance to the anti-estrogens tamoxifen or ICI-182,780 (Figure 3A). Depicted is the maximal alteration in FRET ratio, as shown in Figure 2. We tested various factors associated with ligand-independent transactivation of ER, including SRC-1 (steroid receptor cofactor-1) (7), cyclin D1 (8), and cAMP (4). As indicated in Figure 3A, membrane-permeable 8-Br-cAMP (33) prevented tamoxifen-associated FRET changes in YFP-ER-CFP transfected U2OS cells, whereas 8-Br-cAMP in

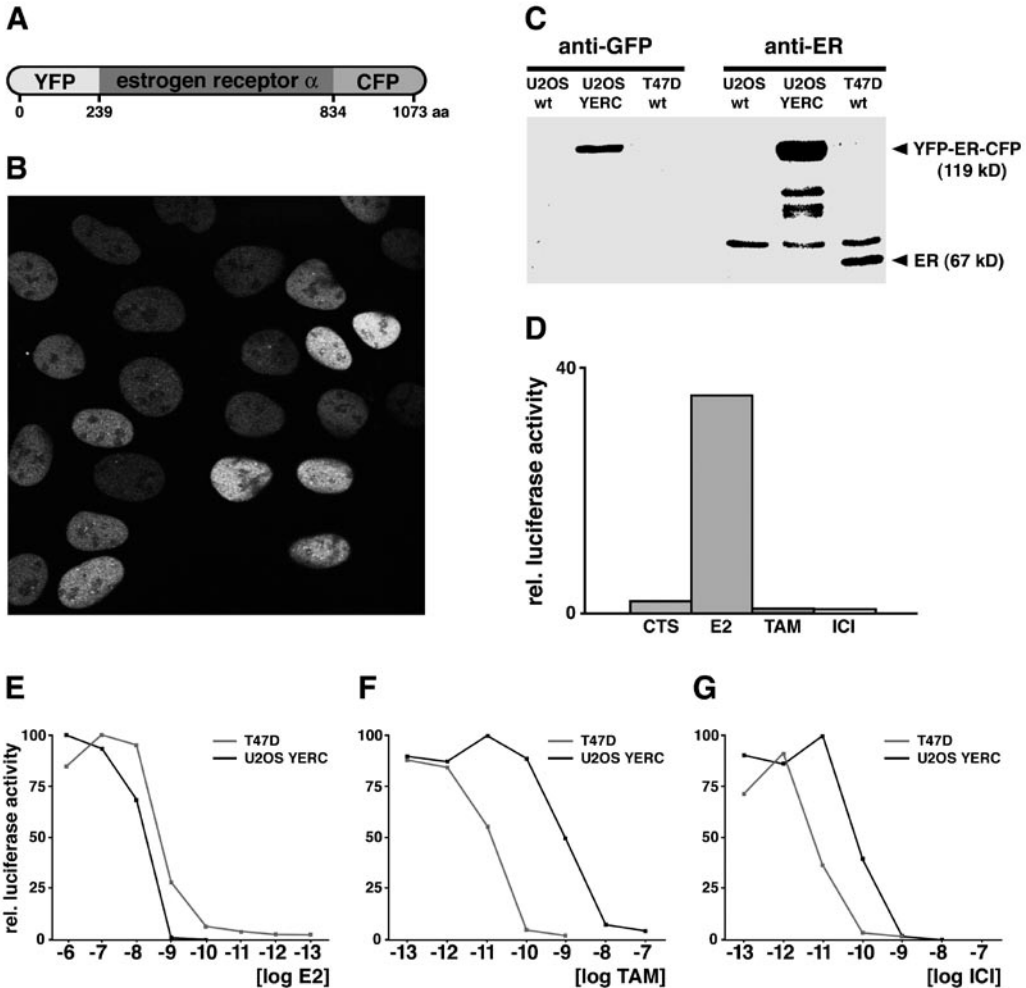


Figure 1. Characterization of YFP-ER-CFP-expressing U2OS cells. **(A)** Scheme of the fusion protein of ER α with YFP at the N-terminus and CFP at the C-terminus. **(B)** Distribution of YFP-ER α -CFP in transiently transfected U2OS cells. Confocal microscopy showed cells with YFP-positive nuclei. **(C)** Western blot analysis. A 119 kDa fusion protein of YFP-ER-CFP was detected by antibodies to GFP and ER in transfected U2OS cells. The 67 kDa wt-ER α was detected by anti-ER antibody in T47D breast cancer cells. **(D)** ERE-dependent luciferase activity in the presence of medium with 5% CTS (charcoal treated serum), 10^{-7} M E2, 10^{-7} M 4-OH-tamoxifen (TAM), or 10^{-7} M ICI-182,780 (ICI). **(E)** ERE-dependent luciferase activity of T47D breast cancer cells containing wt ER and U2OS cells containing YFP-ER α -CFP in the presence of various concentrations of E2. **(F)** and **(G)** ERE-dependent luciferase activity of T47D breast cancer cells containing wt ER and U2OS cells containing YFP-ER α -CFP in the presence of 10^{-8} M E2 (T47D cells) or 3×10^{-9} M E2 (U2OS containing YFP-ER α -CFP cells) in the presence of various concentrations of OH-tamoxifen **(F)** or ICI-182,780 **(G)**.

combination with cyclin D1 and SRC-1 was required to overcome the ICI-182,780-induced FRET change. Without 8-Br-cAMP, overexpression of cyclin D1 and SRC-1, either alone or in combination, was not sufficient to overcome the tamoxifen or ICI-182,780-induced FRET change. ERE-dependent luciferase

assays in U2OS cells were used to confirm that the changes in FRET were associated with inhibition of ER and subsequent reduction of ER transactivation, whereas resistance to anti-estrogens was associated with no alteration in FRET and with ER transactivation in the presence of anti-estrogens (Figure 3B).

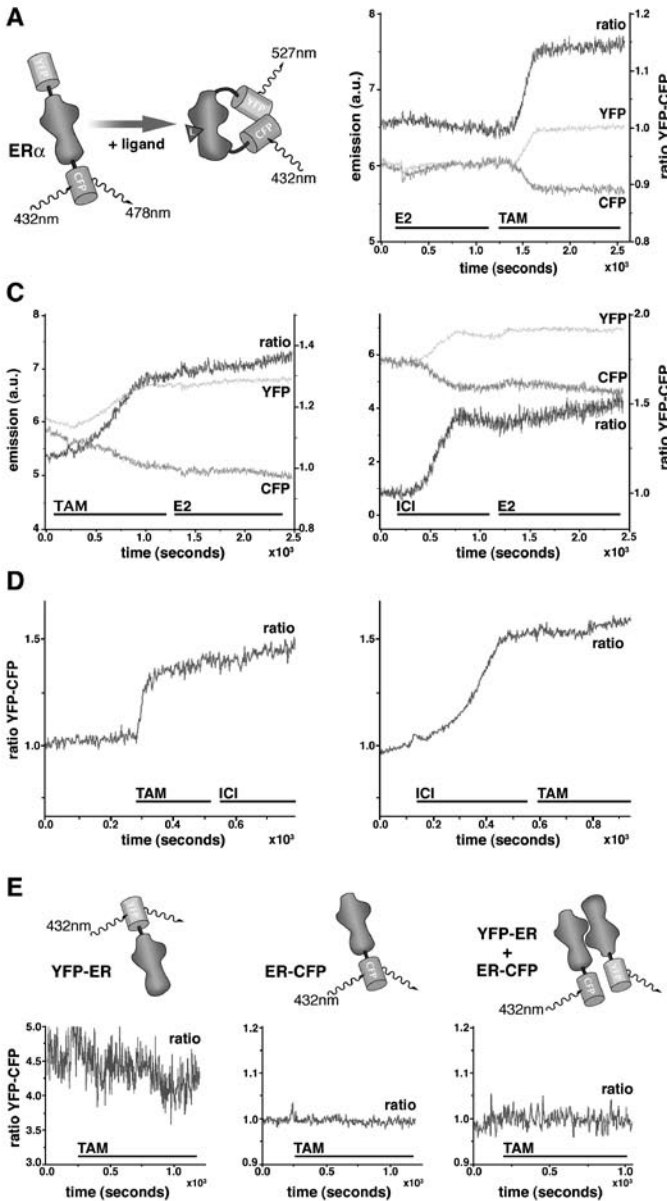


Figure 2. Visualization of ER α inactivation by anti-estrogens using FRET.

(A) Principle of FRET. Exciting CFP at 432 nm results in emission at 478 nm unless energy is transferred to YFP. An increased YFP (at 527 nm) can occur as the result of a conformational change of ER.

(B) FRET change induced by tamoxifen. Time course of emission of YFP (yellow) and CFP (blue) and corresponding ratio of YFP/CFP emission (red) of one YFP-ER-CFP-containing U2OS cell after subsequent addition of 10^{-7} M estradiol (E2) and 10^{-6} M 4-OH-tamoxifen (TAM), as indicated.

(C) Time course of YFP/CFP emission ratio of one YFP-ER-CFP-containing U2OS cell after subsequent addition of 10^{-7} M 4-OH-tamoxifen (TAM) (left) or 10^{-7} M ICI-182,780 (ICI) (right) followed by addition of 10^{-6} M estradiol (E2), as indicated.

(D) Time course of YFP/CFP emission ratio of one YFP-ER-CFP-containing U2OS cell cultured in the presence of 10^{-7} M 4-OH-tamoxifen (TAM) and 10^{-6} M ICI-182,780 (ICI), as indicated (left), or with the same compounds in the reversed order (right).

(E) FRET detects an intramolecular change in ER α . Time course of YFP/CFP emission ratio of one U2OS cells expressing YFP-ER (left), ER-CFP (middle), or both YFP-ER and ER-CFP (right). The cells were cultured in CTS-containing medium followed by addition of 10^{-7} M 4-OH-tamoxifen (TAM).

Administration of 8-Br-cAMP resulted in a 5.5-fold increase of the basal activity of the reporter construct under CTS conditions alone (Figure 3B) that is not accompanied by a FRET change. Only anti-estrogens induce a conformational change that results in a FRET alteration.

Next, we applied FRET to investigate the mechanism of resistance toward anti-estrogens induced

by 8-Br-cAMP. This compound overcomes the tamoxifen- but not ICI-182,780-induced inactivation of ER, a situation often observed with tamoxifen-resistant patients as well (20, 22). cAMP is generated by adenylate cyclase activity, which can be stabilized by forskolin, and activates protein kinase A (PKA). When added to the YFP-ER-CFP transfected U2OS cells 15 min before anti-estrogen administration, forskolin prevented tamoxifen-, but not the ICI-182,780-

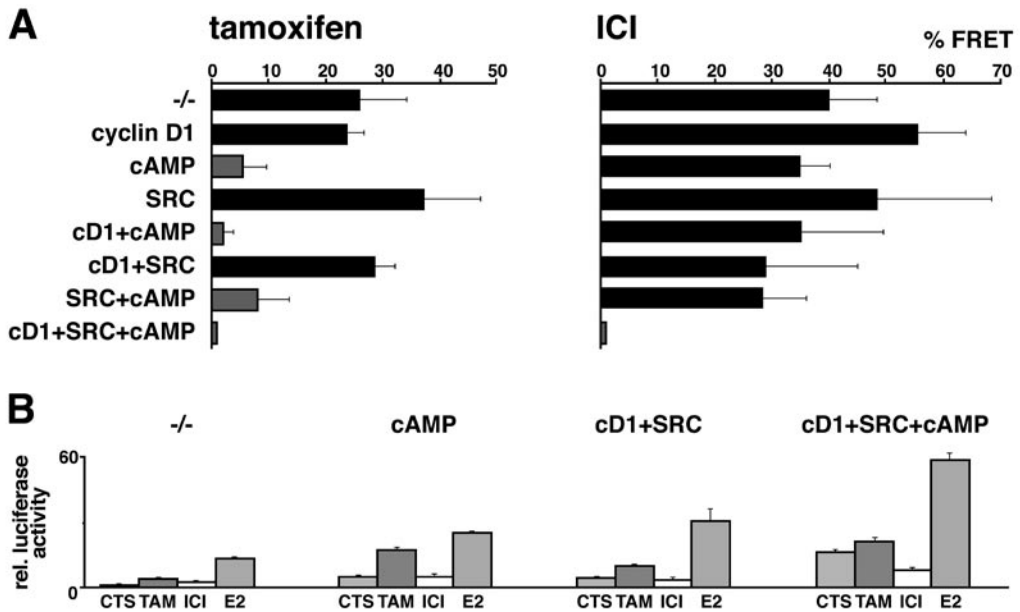


Figure 3. Manipulation of tamoxifen-induced inactivation of ER α (A) FRET values (shown as maximal percentage alteration in FRET ratio) in YFP-ER-CFP-expressing U2OS cells after addition of 10^{-7} M 4-OH-tamoxifen or 10^{-7} M ICI-182,780 to control cells (-/-), cells expressing either cyclin D1 or SRC-1, cells pretreated with 8Br-cAMP (cAMP), or cells containing various combinations as indicated. Bars indicate the standard error in at least four independent experiments. (B) ER transcriptional activity measured by ERE-dependent luciferase assay under the same conditions as in A. Cells were cultured for two days in the presence of either CTS medium, 10^{-7} M 4-OH-tamoxifen (TAM), or 10^{-7} M ICI-182,780 (ICI) and subsequently assayed by the ERE-luciferase assay as described in Experimental Procedures. Bars indicate standard error in triplicate experiments.

induced, FRET change (Figures 4B and 4C). Again, these findings were confirmed in ER-mediated transactivation experiments in the presence of 8Br-cAMP (Figure 3B). Surprisingly, addition of a 10-fold molar excess of ICI-182,780 after tamoxifen treatment did not result in a FRET change (Figure 4B). The estrogen binding site in ER α was apparently occupied by tamoxifen, thus preventing an ICI-182,780-induced FRET change. The reverse was also true: tamoxifen could not alter the ICI-induced conformational change as visualized by FRET (Figure 4C). Since ICI-182,780 substitution for tamoxifen was not observed in our experiments (up to 120 min), this indicated that anti-estrogens had a very low off-rate after ER binding. After PKA activation, tamoxifen failed to induce the inactive state of ER α , as measured by FRET (Figure 4B), but instead induced ER-dependent transcription, as also visualized by the transactivation experiments (Figure 3B). PKA activation thus converted tamoxifen from an antagonist into an agonist.

There are two consensus PKA phosphorylation sites in ER α , one within the DNA binding domain (serine-236) and a second at the N-terminal boundary of the ligand binding E domain, near the hinge region (serine-305) (34). Mutation of serine-236 to alanine had a partial effect (data not shown). Mutation of serine-305 to alanine, however, completely prevented the effect of forskolin on the tamoxifen induced, but not on the ICI-182,780-induced FRET change (Figure 4D). Serine 305 of ER α also appeared to be a *bona fide* target of PKA activity in an *in vitro* kinase assay (Figure 4E). The ER α ser \rightarrow ala 236 mutant protein was efficiently phosphorylated, whereas the ser \rightarrow ala 305 was not, indicating that not the ser-236 but rather the ser-305 site in ER α is the main target of PKA activity. We performed these kinase experiments *in vitro* to exclude activation/involvement of other kinases. PKA thus rendered ER α resistant to tamoxifen by phosphorylation of serine-305 in the hinge region.

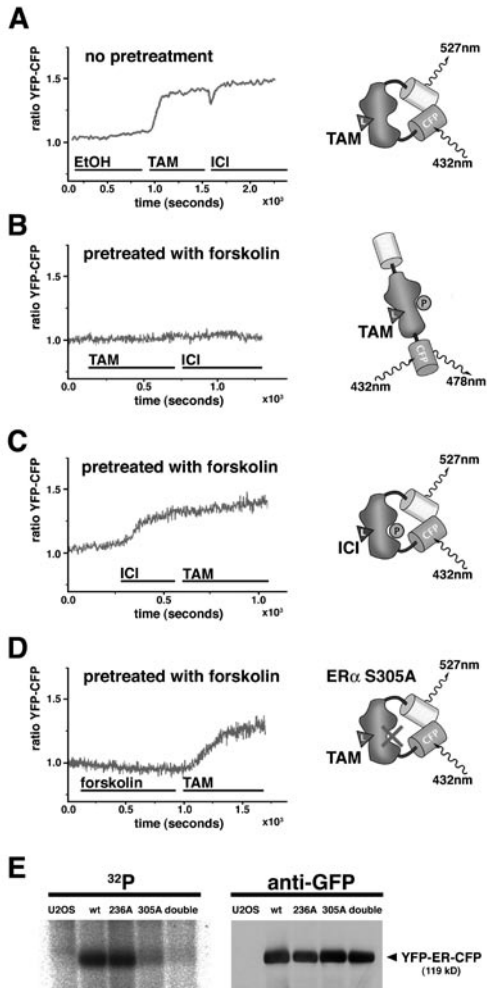


Figure 4. Forskolin treatment selectively prevents tamoxifen-induced inactivation of ER α (A–D) Time course of YFP/CFP ratio of a YFP-ER α -CFP-expressing U2OS cell cultured either in CTS medium (top) or treated with 10^{-5} M forskolin for 15 min prior to FRET measurement (B–D). Subsequently, 10^{-7} M 4-OH-tamoxifen (TAM) and 10^{-6} M ICI-182,780 (ICI) (B) or in the reversed order (10^{-7} M ICI and 10^{-6} M TAM) (C) was added, as indicated. The right panel shows the molecular interpretation of the FRET experiments. (D) Phosphorylation of serine-305 by PKA renders ER α resistant to tamoxifen. Time course of YFP/CFP ratio of an YFP-ER α (305A)-CFP expressing U2OS cell cultured in CTS and treated with 10^{-5} M forskolin for 15 min prior to FRET measurement. Subsequently, 10^{-6} M 4-OH-tamoxifen (TAM) was added. (E) *In vitro* phosphorylation of serine 305 by PKA. Equal amounts of protein of wt and Ser \rightarrow Ala 236 and/or -305 mutants of GFP-immunopurified YFP-ER α -CFP were incubated with protein kinase A and γ^{32} P-ATP, and the reactions were evaluated by autoradiography after gelectrophoresis and Western blotting using antibody against GFP as described in the Experimental Procedures. Total U2OS protein was used as control.

Supplemental Tables S1 and S2 at <http://www.cancer-cell.org/cgi/content/full/5/6/597/DC1>. The expression profile of each tumor was analyzed using a pool of tumors as a reference. The association of expression of the different genes within the PKA pathway with tamoxifen sensitivity was evaluated by correlation of the average expression of each gene with the outcome of disease (32). Only expression of the negative regulatory subunit of PKA, PKA-R1 α , was found to be significantly reduced in tamoxifen-resistant breast tumors, whereas other components of the PKA pathway were not involved (Table 1 and Supplemental Data). Among the 100 genes whose altered expression was associated with tamoxifen resistance, no gene involved in the MAP kinase pathway was found to be associated with tamoxifen resistance. Also, neither SRC-1 nor cyclin D1 was found to be associated with tamoxifen resistance, which is consistent with our FRET data that PKA activation alone (by cAMP) renders ER α resistant to tamoxifen. To substantiate the relevance of reduced expression of PKA-R1 α , we downregulated PKA-R1 α in the YFP-ER-CFP cells in our experimental system by RNAi (Figure 5A, insert). FRET analysis of U2OS cells cotransfected with the PKA-R1 α RNAi construct showed no alteration in FRET upon tamoxifen treatment, whereas ICI-182,780 did induce a FRET change (Figure 5A). Again, addition of a ten-fold molar excess of ICI-182,780 after tamoxifen treatment did not yield a

PKA-R1 α and resistance to tamoxifen

We studied the relevance of PKA activation for tamoxifen resistance in 70 ER+ primary breast cancers that were isolated before tamoxifen treatment, of which 20 patients showed recurrence of the tumor. These primary tumors were consequently classified as tamoxifen-resistant. The remaining 50 patients showed no recurrence in the form of metastasis after an average follow-up period of 132 months, which classified these tumors as potentially tamoxifen-sensitive. However, the nonrecurrent group may have contained tamoxifen-resistant cases that did not show recurrence because of the absence of micrometastases. The clinical details of the patient groups and the microarray approach used in this study are given in

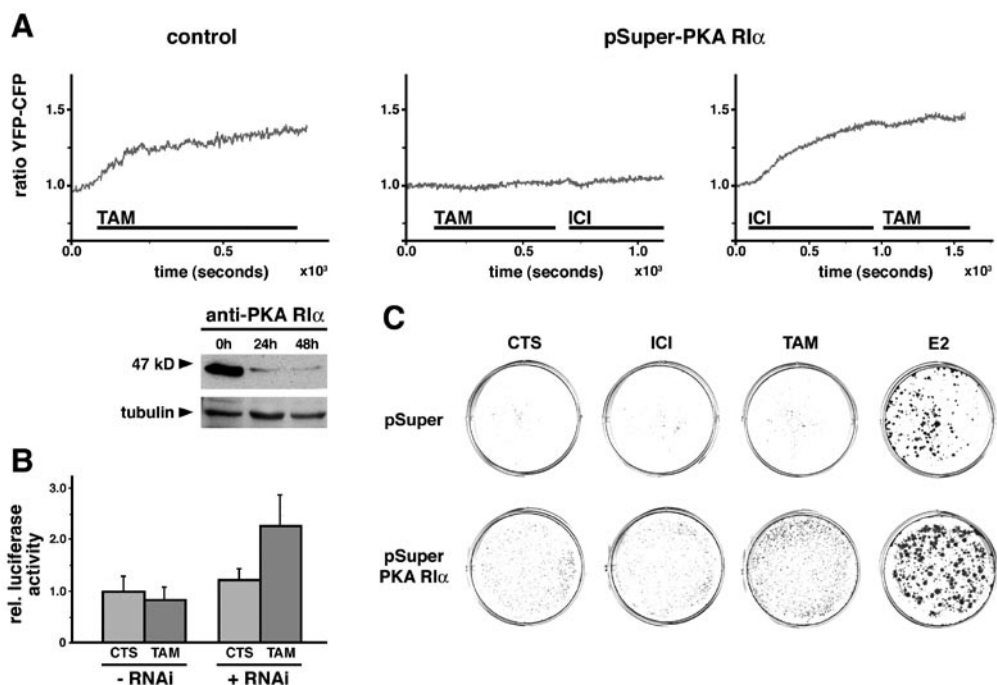


Figure 5. Reduced expression of the negative regulatory subunit of PKA, PKA-R1 α , results in tamoxifen resistance and induces breast cancer growth. **(A)** Reduced expression of PKA-R1 α by RNAi results in tamoxifen resistance, but not ICI-182,780 resistance. Time course of YFP/CFP ratio of a YFP-ER-CFP expressing U2OS cell. 10^{-7} M 4-OH-tamoxifen (TAM) was added in the control experiment (left panel). Alternatively, cells were cotransfected with PKA-R1 α -RNAi, which considerably reduced expression of PKA-R1 α , as determined by Western blot analysis (insert). These cells were subsequently treated with 10^{-7} M 4-OH-tamoxifen (TAM) and 10^{-6} M ICI-182,780 (ICI) (middle), or in the reversed order (right panel), as indicated. **(B)** ER transactivation determined by ERE-luciferase activity of control U2OS cells transfected with YFP-ER-CFP alone (-RNAi), and cells cotransfected with PKA-R1 α -RNAi (+RNAi). Cells were cultured in CTS medium or in CTS medium containing 10^{-7} M 4-OH-tamoxifen (TAM) for two days. **(C)** Reduced expression of PKA-R1 α by RNAi results in tamoxifen resistant- but not ICI-182,780-resistant proliferation. Electroporation of pSuper-PKA-R1 α DNA (1 μ g) or control empty vector (pSuper) into 100,000 single T47D cells and subsequent culturing of these in the presence of either CTS medium, 10^{-7} M ICI-182,780 (ICI), 10^{-7} M 4-OH-tamoxifen (TAM), or 10^{-7} M E2 for three weeks resulted in tamoxifen-resistant proliferation. Coomassie blue staining of the resulting colonies is shown.

FRET change, whereas addition of these compounds in the reverse order did show the regular ICI-182,780-associated FRET alteration. Tamoxifen resistance of ER α after PKA activation — through downregulation of PKA-R1 α — was confirmed in traditional ER-dependent transactivation assays that were performed in U2OS cells (**Figure 5B**) and in *in vitro* proliferation experiments, where ER-positive T47D breast cancer cells were used (**Figure 5C**). For FRET and ER-reporter assays, we used U2OS cells that are easily transfectable, but are not dependent on estrogen for their growth when transfected with ER α (35). In contrast, growth of ER-positive T47D breast cancer cells is estrogen-dependent, and can be inhibited by anti-

estrogens. When T47D cells were transfected with PKA-R1 α RNAi, however, they continued to proliferate in the presence of tamoxifen, but not with ICI 182,780. Activation of PKA by RNAi for PKA-R1 α induced protein expression of a progesterone receptor related protein of 140 kDa that is normally induced by E2 only (data not shown). This suggests that tamoxifen-bound ER α can act as a transcriptional activator, like E2-bound ER α , after modification by PKA, as indicated by the transactivation reporter assays as well (**Figure 5B**). T47D cells transfected with an empty vector ceased to proliferate in the presence of these anti-estrogens (**Figure 5C**). Elevated PKA activity (by reduction of PKA-R1 α) resulted in increased

	Gene	Non- Recurrent _a	Recurrent _b	P-value _c
Protein kinase A (PKA)-catalytic subunits				
alpha 1	PRKAA1	- 0.009	- 0.108	0.191
beta	PRKACB	- 0.363	- 0.242	0.454
gamma	PRKACG	0.149	0.202	0.267
Protein kinase A (PKA)-non-catalytic, AMP activated subunits				
beta 1	PRKAB1	- 0.025	0.150	0.141
beta 2	PRKAB2	- 0.006	-0.004	0.974
gamma 1	PRKAG1	0.007	- 0.101	0.403
gamma 2	PRKAG2	0.024	0.056	0.490
Protein kinase A (PKA)-non-catalytic, cAMP dependent, regulatory subunits				
type I, alpha 1	PRKAR1A	- 0.102	- 0.469	0.000
type I, beta	PRKAR1B	0.212	0.039	0.610
type II, alpha	PRKAR2A	0.023	0.056	0.597
type II, beta	PRKAR2B	- 0.113	- 0.108	0.224

Table 1. Reduced expression of PKA-R1α is associated with tamoxifen resistance. Association between expression of PKA-pathway related genes and recurrence of breast cancers after tamoxifen treatment. The expression of PKA-pathway related genes was determined in 70 breast tumors that were surgically removed prior to tamoxifen treatment. Expression levels were determined using a pool of 56 randomly chosen breast tumors from this series as a reference, as indicated in Experimental Procedures. a: mean log2 value of the gene expression in the non-recurrent group of breast cancers. b: mean log2 value of gene expression in the recurrent group of breast cancers. c: P-value of Wilcoxon rank sum test between recurrent and non-recurrent group of breast cancers. A significant difference is given by a P value <0.05. The gene expression that significantly differed between the non-recurrent and recurrent group is marked in bold.

Hormone condition	T47D transfected with:		
	pSuper	pSuper PKA-R1α	ratio
CTS	0.96±0.29	4.46±0.68	4.66
10 ⁻⁷ M ICI 182,780	0.76±0.22	3.46±0.11	4.55
10 ⁻⁷ M OH-TAM	1.04±0.39	8.58±2.04	8.69
10 ⁻⁷ M E2	10.02±0.38	33.78±3.01	3.37

Table 2. Colony density of T47D breast cancer cells transfected with PKA-R1α RNAi pSuper or with pSuper alone and cultured for three weeks under various hormonal conditions. After Coomassie blue staining, the density of the colonies presented in Figure 5C was measured as described by Brummelkamp et al. (29), and is given in arbitrary units.

E2-driven proliferation as well, comparable to the increased ER transactivation measured by ERE luciferase activity under those conditions (Figure 3B), as has also been reported previously (34). Quantitation of colony densities of T47D cells with reduced levels of PKA-R1α as compared to controls indicated that growth in tamoxifen conditions exceeded that in conditions of ICI-182,780 or hormone ablation by approximately 2-fold, implying that both downregulation of PKA-R1α and tamoxifen were required for the increased cell growth (Table 2). Evidently, downregulation of PKA-R1α resulted in activation of the PKA pathway and induced selective tamoxifen resistance not only under experimental conditions, but also in breast cancer patients. Under these conditions, tamoxifen binds to ERα, but cannot induce the inhibitory conformation. Even more important, tamoxifen is now activating ER-controlled transcription and tumor cell growth.

Discussion

Here we show that PKA activation sufficed to induce tamoxifen resistance in breast cancer. In principle, this can be achieved by alteration of one or more steps within the PKA pathway (Figure 6). However, constitutive activation of PKA is difficult to achieve through G protein-coupled receptors or adenylate cyclase, because these receptors are desensitized after activation. Yet alteration can be achieved by overexpression of PKA or downregulation of the inhibitory subunit PKA-R1α, of which the latter occurred in most of the primary breast tumors that appear resistant to subsequent tamoxifen treatment (Table 1). Obviously, we cannot exclude additional mechanisms for inducing tamoxifen resistance. Our experimental RNAi approach, however, showed that reduction of PKA-R1α alone was sufficient to induce tamoxifen resistance. Downregulation of PKA-R1α in breast tumor sections has already been associated with tamoxifen resistance (36), but here we directly implicate this protein as a causative factor in this process and describe the mechanism of its action. By combining biophysical techniques (FRET) with microarray and RNAi technology, we have implicated the PKA pathway in tamoxifen resistance, not only in tissue culture cells, but also in breast cancer patients, and have identified ERα serine-305 as the critical target site. Interestingly, this site is located near the hinge region of ERα. Our FRET findings indicated that tamoxifen is able to bind to a PKA modified ERα (Figures 4B and 4C).

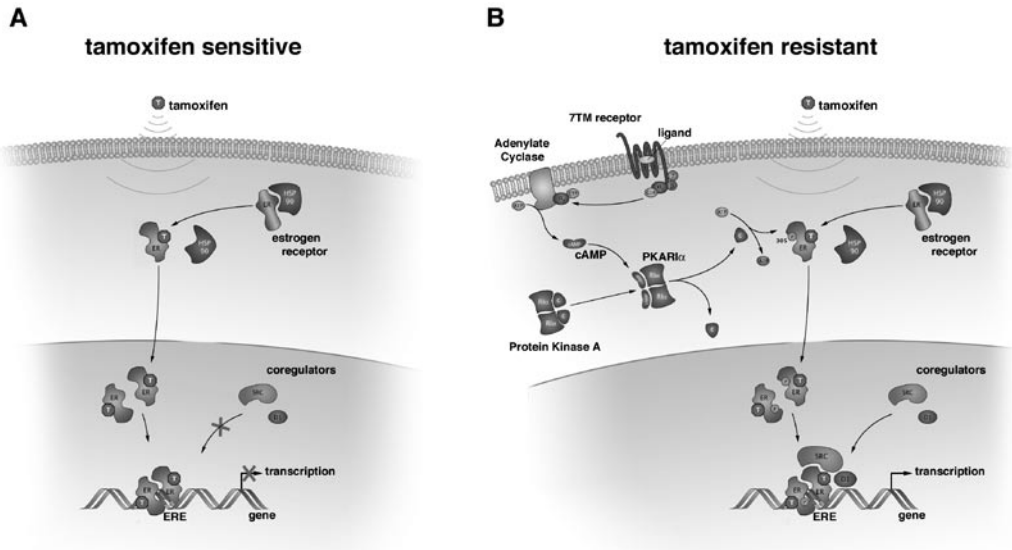


Figure 6. Model for PKA-mediated resistance to tamoxifen. ER α -complex binds to its cognate ERE recognition site in the promoter of estrogen responsive genes. Transcription is mediated through the subsequent recruitment of a number of coactivators, an interaction stabilized by cyclin D1. **(A)** Nonresistant cells. The binding of tamoxifen (T) to ER prevents the recruitment of coactivator SRC-1 and impedes ER-mediated transcription. **(B)** Tamoxifen-resistant cells. Activation of PKA prevents tamoxifen-mediated inhibition of ER transactivation. The PKA pathway can be activated by ligand binding to a G protein-coupled receptor (7TM receptor). G proteins subsequently activate adenylate cyclase that generates cAMP. Adenylate cyclase activity is stabilized by forskolin. cAMP binding to the catalytic subunit of the PKA complex releases the inhibitory subunit PKA-R1 α from the PKA complex. The catalytic PKA subunit (c) now phosphorylates serine-305 of ER α and thus blocks conversion into its inactive conformation by tamoxifen. In fact, tamoxifen now promotes ER α induced transcription and proliferation of hormone-dependent breast tumor cells. Reduction in expression of PKA-R1 α , as observed in many tamoxifen-resistant breast cancer patients or by RNAi, also results in PKA activation and tamoxifen resistance. Phosphorylation of Ser-305 of ER α then controls the switch from inhibition to growth stimulation by tamoxifen.

Phosphorylation of serine-305 by PKA therefore appears to affect the stability of the conformation of ER α upon anti-estrogen binding rather than the binding properties of the receptor itself. FRET also revealed that tamoxifen induced resistance through a unique mechanism; PKA modified the ER α such that tamoxifen still bound to but was unable to convert the receptor into an inactive conformation. As a result, tamoxifen activated ER-mediated transcription and now acted as an agonist instead of an antagonist. This modification led to a specific tamoxifen-resistant proliferation, whereas sensitivity to ICI-182,780 remained unaltered. The stabilized conformation of ER α might lead to either enhanced recruitment of cofactors, such as SRC-1, or to reduced binding of corepressors, such as NCoR. These factors are subject to modification of PKA themselves, which may contribute to recruitment/dissemination by/from ER α that is modified by PKA (37). Resistance to ICI-182,780

was only achieved when additional factors, such as overexpression of SRC1 and cyclin D1, were involved (Figure 3). In that case, it is likely that overexpression of cofactor SRC1 and cyclin D1 helped to stabilize the interaction between SRC1 and ER α , consolidating the PKA-induced conformational change in ER α even further. This resulted to an active conformation of ER α also in the presence of ICI-182,780, as measured by FRET. It is known that tamoxifen can act both as ER antagonist and agonist—antagonistic in breast tissue, while agonistic in a number of other tissues, such as osteoblasts (38). For this reason, tamoxifen has beneficial effects on osteoporosis by stimulating ER α -dependent proliferation of osteoblasts. Why tamoxifen induces opposite effects in different tissues is unclear. Overexpression of SRC-1 has been claimed to be one factor (7). However, our data showed that this did not suffice to convert the antagonistic effects of tamoxifen into an agonistic effect, unless PKA was

activated as well. The activity of PKA may therefore be the critical factor. This is highly relevant for breast cancer patients, since tamoxifen may induce the opposite effect when PKA is activated, stimulating ER α -dependent tumor growth rather than inhibiting it. Indeed, this situation is encountered in the clinic in the “withdrawal response,” where tamoxifen-resistant breast tumor ceases to grow upon withdrawal of tamoxifen (39). This counterintuitive effect of tamoxifen can be understood from our observations where tamoxifen is converted from an inhibitor into a growth stimulator when the estrogen receptor α is

phosphorylated at position 305 by PKA. Patients who are potentially resistant to tamoxifen should be identified and treated with unequivocal ER antagonists such as ICI-182,780 (Fulvestrant). Indeed, 45% of the tamoxifen-resistant breast cancer patients respond favorably to treatment with Fulvestrant (21).

Acknowledgements

We thank Wouter Moolenaar, Anton Berns, and Helen Pickersgill for critical reading of the manuscript, and Piet Borst for valuable comments.

References

- Bryant, P.W., et al., Proteolysis and antigen presentation by MHC class II molecules. *Adv Immunol*, 2002. 80: p. 71-7114.
- Peters, P.J., et al., Segregation of MHC class II molecules from MHC class I molecules in the Golgi complex for transport to lysosomal compartments. *Nature*, 1991. 349(6311): p. 669-676.
- Cresswell, P., Chemistry and functional role of the invariant chain. *Curr Opin Immunol*, 1992. 4(1): p. 87-92.
- Denzin, L.K. and P. Cresswell, HLA-DM induces CLIP dissociation from MHC class II alpha beta dimers and facilitates peptide loading. *Cell*, 1995. 82(1): p. 155-165.
- Kropshofer, H., et al., HLA-DM acts as a molecular chaperone and rescues empty HLA-DR molecules at lysosomal pH. *Immunity*, 1997. 6(3): p. 293-302.
- Sherman, M.A., D.A. Weber, and P.E. Jensen, DM enhances peptide binding to class II MHC by release of invariant chain-derived peptide. *Immunity*, 1995. 3(2): p. 197-205.
- Chou, C.L. and S. Sadegh-Nasseri, HLA-DM recognizes the flexible conformation of major histocompatibility complex class II. *J Exp Med*, 2000. 192(12): p. 1697-1706.
- Sanderson, F., et al., Association between HLA-DM and HLA-DR *in vivo*. *Immunity*, 1996. 4(1): p. 87-96.
- Vogt, A.B., et al., Quality control of MHC class II associated peptides by HLA-DM/H2-M. *Semin Immunol*, 1999. 11(6): p. 391-403.
- Doebele, R.C., et al., Determination of the HLA-DM interaction site on HLA-DR molecules. *Immunity*, 2000. 13(4): p. 517-527.
- Pashine, A., et al., Interaction of HLA-DR with an acidic face of HLA-DM disrupts sequence-dependent interactions with peptides. *Immunity*, 2003. 19(2): p. 183-192.
- Ullrich, H.J., et al., Interaction between HLA-DM and HLA-DR involves regions that undergo conformational changes at lysosomal pH. *Proc Natl Acad Sci U S A*, 1997. 94(24): p. 13163-13168.
- Denzin, L.K., et al., Negative regulation by HLA-DO of MHC class II-restricted antigen processing. *Science*, 1997. 278(5335): p. 106-109.
- Liljedahl, M., et al., Altered antigen presentation in mice lacking H2-O. *Immunity*, 1998. 8(2): p. 233-243.
- van Ham, S.M., et al., HLA-DO is a negative modulator of HLA-DM-mediated MHC class II peptide loading. *Curr Biol*, 1997. 7(12): p. 950-957.
- Calafat, J., et al., Major histocompatibility complex class II molecules induce the formation of endocytic MIIC-like structures. *J Cell Biol*, 1994. 126(4): p. 967-977.
- Kleijmeer, M.J., et al., Major histocompatibility complex class II compartments in human and mouse B lymphoblasts represent conventional endocytic compartments. *J Cell Biol*, 1997. 139(3): p. 639-649.
- Gruenberg, J., Lipids in endocytic membrane transport and sorting. *Curr Opin Cell Biol*, 2003. 15(4): p. 382-388.
- Wubbolts, R., et al., Proteomic and biochemical analyses of human B cell-derived exosomes. Potential implications for their function and multivesicular body formation. *J Biol Chem*, 2003. 278(13): p. 10963-10972.
- Escola, J.M., et al., Selective enrichment of tetraspan proteins on the internal vesicles of multivesicular endosomes and on exosomes secreted by human B-lymphocytes. *J Biol Chem*, 1998. 273(32): p. 20121-20127.
- Hammond, C., et al., The tetraspan protein CD82 is a resident of MHC class II compartments where it associates with HLA-DR, -DM, and -DO molecules. *J Immunol*, 1998. 161(7): p. 3282-3291.
- Kropshofer, H., et al., Tetraspan microdomains distinct from lipid rafts enrich select peptide-MHC class II complexes. *Nat Immunol*, 2002. 3(1): p. 61-68.
- Katzmann, D.J., G. Odorizzi, and S.D. Emr, Receptor downregulation and multivesicular-body sorting. *Nat Rev Mol Cell Biol*, 2002.

- 3(12): p. 893-905.
24. Fernandez-Borja, M., et al., Multivesicular body morphogenesis requires phosphatidylinositol 3-kinase activity. *Curr Biol*, 1999. 9(1): p. 55-58.
 25. Morrison, L.A., et al., Differences in antigen presentation to MHC class I-and class II-restricted influenza virus-specific cytolytic T lymphocyte clones. *J Exp Med*, 1986. 163(4): p. 903-921.
 26. Song, W., et al., Wortmannin, a phosphatidylinositol 3-kinase inhibitor, blocks the assembly of peptide-MHC class II complexes. *Int Immunol*, 1997. 9(11): p. 1709-1722.
 27. Brumell, J.H. and S. Grinstein, Salmonella redirects phagosomal maturation. *Curr Opin Microbiol*, 2004. 7(1): p. 78-84.
 28. Russell, D.G., Phagosomes, fatty acids and tuberculosis. *Nat Cell Biol*, 2003. 5(9): p. 776-778.
 29. Harding, C.V., L. Ramachandra, and M.J. Wick, Interaction of bacteria with antigen presenting cells: influences on antigen presentation and antibacterial immunity. *Curr Opin Immunol*, 2003. 15(1): p. 112-119.
 30. Ramachandra, L., et al., Processing of *Mycobacterium tuberculosis* antigen 85B involves intraphagosomal formation of peptide-major histocompatibility complex II complexes and is inhibited by live bacilli that decrease phagosome maturation. *J Exp Med*, 2001. 194(10): p. 1421-1432.
 31. Ullrich, H.J., W.L. Beatty, and D.G. Russell, Interaction of *Mycobacterium avium*-containing phagosomes with the antigen presentation pathway. *J Immunol*, 2000. 165(11): p. 6073-6080.
 32. Vergne, I., J. Chua, and V. Deretic, Tuberculosis toxin blocking phagosome maturation inhibits a novel Ca_2^+ /calmodulin-PI3K hVPS34 cascade. *J Exp Med*, 2003. 198(4): p. 653-659.
 33. Hernandez, L.D., et al., Salmonella modulates vesicular traffic by altering phosphoinositide metabolism. *Science*, 2004. 304(5678): p. 1805-1807.
 34. Stam, N.J., H. Spits, and H.L. Ploegh, Monoclonal antibodies raised against denatured HLA-B locus heavy chains permit biochemical characterization of certain HLA-C locus products. *J Immunol*, 1986. 137(7): p. 2299-2306.
 35. Vennegoor, C. and P. Rumke, Circulating melanoma-associated antigen detected by monoclonal antibody NK1/C-3. *Cancer Immunol Immunother*, 1986. 23(2): p. 93-100.
 36. Adams, T.E., J.G. Bodmer, and W.F. Bodmer, Production and characterization of monoclonal antibodies recognizing the alpha-chain subunits of human Ia alloantigens. *Immunology*, 1983. 50(4): p. 613-24.
 37. Shaw, S., A. Ziegler, and R. DeMars, Specificity of monoclonal antibodies directed against human and murine class II histocompatibility antigens as analyzed by binding to HLA-deletion mutant cell lines. *Hum Immunol*, 1985. 12(4): p. 191-211.
 38. Neeffjes, J.J., et al., The biosynthetic pathway of MHC class II but not class I molecules intersects the endocytic route. *Cell*, 1990. 61(1): p. 171-83.
 39. van Ham, S.M., et al., HLA-DO is a negative modulator of HLA-DM-mediated MHC class II peptide loading. *Curr Biol*, 1997. 7(12): p. 950-7.
 40. Morton, P.A., et al., Delivery of nascent MHC class II-invariant chain complexes to lysosomal compartments and proteolysis of invariant chain by cysteine proteases precedes peptide binding in B-lymphoblastoid cells. *J Immunol*, 1995. 154(1): p. 137-50.
 41. Copier, J., et al., Targeting signal and subcellular compartments involved in the intracellular trafficking of HLA-DMB. *J Immunol*, 1996. 157(3): p. 1017-27.
 42. van Ham, M., et al., Modulation of the major histocompatibility complex class II-associated peptide repertoire by human histocompatibility leukocyte antigen (HLA)-DO. *J Exp Med*, 2000. 191(7): p. 1127-36.
 43. Marks, M.S., et al., A lysosomal targeting signal in the cytoplasmic tail of the beta chain directs HLA-DM to MHC class II compartments. *J Cell Biol*, 1995. 131(2): p. 351-69.
 44. Nijenhuis, M., et al., Targeting major histocompatibility complex class II molecules to the cell surface by invariant chain allows antigen presentation upon recycling. *Eur J Immunol*, 1994. 24(4): p. 873-83.
 45. Kanda, T., K.F. Sullivan, and G.M. Wahl, Histone-GFP fusion protein enables sensitive analysis of chromosome dynamics in living mammalian cells. *Curr Biol*, 1998. 8(7): p. 377-85.
 46. Brummelkamp, T.R., R. Bernards, and R. Agami, A system for stable expression of short interfering RNAs in mammalian cells. *Science*, 2002. 296(5567): p. 550-3.
 47. Van Rheenen, J., M. Langeslag, and K. Jalink, Correcting confocal acquisition to optimize imaging of fluorescence resonance energy transfer by sensitized emission. *Biophys J*, 2004. 86(4): p. 2517-29.
 48. Vermeer, J.E., et al., Probing plasma membrane microdomains in cowpea protoplasts using lipidated GFP-fusion proteins and multimode FRET microscopy. *J Microsc*, 2004. 214(Pt 2): p. 190-200.
 49. Boes, M., et al., T-cell engagement of dendritic cells rapidly rearranges MHC class II transport. *Nature*, 2002. 418(6901): p. 983-988.
 50. Wubbolt, R., et al., Direct vesicular transport of MHC class II molecules from lysosomal structures to the cell surface. *J Cell Biol*, 1996. 135(3): p. 611-622.
 51. Marks, M.S., et al., A lysosomal targeting signal in the cytoplasmic tail of the beta chain directs HLA-DM to MHC class II compartments. *J Cell Biol*, 1995. 131(2): p. 351-369.
 52. Germain, R.N. and L.R. Hendrix,

- MHC class II structure, occupancy and surface expression determined by post-endoplasmic reticulum antigen binding. *Nature*, 1991. 353(6340): p. 134-139.
53. Neefjes, J.J. and H.L. Ploegh, Inhibition of endosomal proteolytic activity by leupeptin blocks surface expression of MHC class II molecules and their conversion to SDS resistance alpha beta heterodimers in endosomes. *EMBO J*, 1992. 11(2): p. 411-416.
 54. Förster, T., Zwischenmolekulare Energiewanderung und Fluoreszenz. *Annalen Physik*, 1948. 6: p. 55-75.
 55. Tsien, R.Y., The green fluorescent protein. *Annu Rev Biochem*, 1998. 67: p. 509-544.
 56. Ormo, M., et al., Crystal structure of the *Aequorea victoria* green fluorescent protein. *Science*, 1996. 273(5280): p. 1392-1395.
 57. Mosyak, L., D.M. Zaller, and D.C. Wiley, The structure of HLA-DM, the peptide exchange catalyst that loads antigen onto class II MHC molecules during antigen presentation. *Immunity*, 1998. 9(3): p. 377-383.
 58. Ghosh, P., et al., The structure of an intermediate in class II MHC maturation: CLIP bound to HLA-DR3. *Nature*, 1995. 378(6556): p. 457-462.
 59. van Rheenen, J., M. Langeslag, and K. Jalink, Correcting confocal acquisition to optimize imaging of fluorescence resonance energy transfer by sensitized emission. *Biophys J*, 2004. 86(4): p. 2517-2529.
 60. van Lith, M., et al., Regulation of MHC class II antigen presentation by sorting of recycling HLA-DM/DO and class II within the multivesicular body. *J Immunol*, 2001. 167(2): p. 884-892.
 61. Bastiaens, P.I. and A. Squire, Fluorescence lifetime imaging microscopy: spatial resolution of biochemical processes in the cell. *Trends Cell Biol*, 1999. 9(2): p. 48-52.
 62. Vermeer, J.E.M., et al., Probing plasma membrane microdomains in cowpea protoplasts using lipidated GFP-fusion proteins and multimode FRET microscopy. *J Microsc*, 2004. 214(Pt 2): p. 190-200.
 63. van Ham, M., et al., Modulation of the major histocompatibility complex class II-associated peptide repertoire by human histocompatibility leukocyte antigen (HLA)-DO. *J Exp Med*, 2000. 191(7): p. 1127-1136.
 64. Ohkuma, S. and B. Poole, Cytoplasmic vacuolation of mouse peritoneal macrophages and the uptake into lysosomes of weakly basic substances. *J Cell Biol*, 1981. 90(3): p. 656-664.
 65. Allen, P.M. and E.R. Unanue, Antigen processing and presentation by macrophages. *Am J Anat*, 1984. 170(3): p. 483-490.
 66. Honey, K. and A.Y. Rudensky, Lysosomal cysteine proteases regulate antigen presentation. *Nat Rev Immunol*, 2003. 3(6): p. 472-482.
 67. Sanderson, F., et al., Accumulation of HLA-DM, a regulator of antigen presentation, in MHC class II compartments. *Science*, 1994. 266(5190): p. 1566-1569.
 68. Zur Lage, S., et al., Activation of macrophages and interference with CD4⁺ T-cell stimulation by *Mycobacterium avium* subspecies paratuberculosis and *Mycobacterium avium* subspecies avium. *Immunology*, 2003. 108(1): p. 62-69.
 69. Flynn, J.L. and J. Chan, Immune evasion by *Mycobacterium tuberculosis*: living with the enemy. *Curr Opin Immunol*, 2003. 15(4): p. 450-455.
 70. Beuzon, C.R., et al., pH-dependent secretion of SseB, a product of the SPI-2 type III secretion system of *Salmonella typhimurium*. *Mol Microbiol*, 1999. 33(4): p. 806-816.
 71. Vincent, M.S., J.E. Gumperz, and M.B. Brenner, Understanding the function of CD1-restricted T cells. *Nat Immunol*, 2003. 4(6): p. 517-523.

